

Structure and order parameters in the pressure-induced continuous transition in TeO_2^\dagger

T. G. Worlton and R. A. Beyerlein

Argonne National Laboratory, Argonne, Illinois 60439

(Received 24 June 1974)

Lattice parameters of TeO_2 have been measured from 0 to 32.5 kbar by time-of-flight neutron diffraction. Atomic-position parameters have also been measured to 20 kbar for both the low-pressure tetragonal paratellurite phase and the high-pressure orthorhombic phase, which we determined to have a structure belonging to the $D_2^2(P2_12_12_1)$ space group. We found no hysteresis in the lattice parameters or position parameters in cycling through the transition. We also found that $(b-a)^2/a_0^2$ in the high-pressure phase varied linearly with pressure with a slope of $2.53(1) \times 10^{-4}/\text{kbar}$, going to zero at 9.1 kbar. We detected no discontinuity in volume or the c parameter, but observed anomalies in the slopes dV/dP , $d(a+b)/dP$, and dc/dP . All of these observations are additional experimental evidence for the continuous nature of the transition. The observed D_2^2 structure of the high-pressure phase is a subgroup of order 2 of the D_4^4 paratellurite phase which means that the free energy is an even function of the order parameter, but third-order terms coupling the primary order parameter with secondary or induced order parameters can still be formed. These can be nonzero without affecting the second-order nature of the transition. The primary order parameter $\eta_1 = e_1 - e_2$ and the two induced order parameters which we observed, $\eta_2 = e_1 + e_2$ and $\eta_3 = e_3$, have been used to derive a Landau-like free-energy expansion describing the thermodynamics of the transition. Very little displacement of the Te atoms was observed in going through the transition, but the oxygen atoms underwent large displacements as a function of pressure. There is no change of size of the unit cell at the transition so it is a pure strain transition of the type first discussed by Anderson and Blount.

I. INTRODUCTION

Paratellurite (TeO_2) has a low-velocity acoustic shear mode which propagates along $\langle 110 \rangle$ and corresponds to the effective elastic constant $\frac{1}{2}(C_{11} - C_{12})$. Ultrasonic measurements at high pressure by Percy and Fritz¹ show that $C_{11} - C_{12}$ decreases linearly with pressure, going to zero at a pressure of 9 kbar. The effect of temperature on this pressure-induced transition is slight. Percy and Fritz¹ suggested that the condensation of this vibrational mode gives rise to a second-order transition at $P_c = 9$ kbar and that the resultant static displacements lower the tetragonal symmetry to orthorhombic with a change in point-group symmetry from D_4 to D_2 . Boccara² had previously shown that a condensation of the mode corresponding to $\frac{1}{2}(C_{11} - C_{12})$ would produce this change in point-group symmetry.

We have made neutron-diffraction measurements on TeO_2 at pressures up to 32.5 kbar in order to determine the pressure dependence of the lattice parameters and to determine the structure of the high-pressure phase. The present work shows that the space group changes from the paratellurite $D_4^4(P4_22_12_1)$ structure to the orthorhombic $D_2^2(P2_12_12_1)$ structure. The tetragonal lattice parameter a splits into the unequal a and b orthorhombic lattice parameters, and the quantity $(b-a)^2$ varies linearly with pressure in the high-pressure phase, extrapolating smoothly to

zero at $P_c = 9.1$ kbar. No discontinuities were observed in the volume ($V=abc$) or in the parameters $(a+b)$ or c , but there were discontinuities in the pressure derivatives of these quantities. These observations can be explained in the framework of a Landau-like model³ starting from a series expansion of the strain energy density.⁴ The primary order parameter in the model is associated with the orthorhombic splitting $(b-a)$, while the small discontinuities in slope which were observed for the quantities $(a+b)$ and c reflect the coupling of two secondary order parameters to the primary order parameter.

The elastic powder diffraction measurements also yielded the pressure dependence of the atomic-position parameters and of the Debye-Waller factors. The Te positions showed little variation with pressure and exhibited a small Debye-Waller factor in all cases. The oxygen atoms which are located on $8b$ sites in the tetragonal (D_4^4) phase are on two inequivalent $4a$ sites in the orthorhombic (D_2^2) phase. The displacement of the oxygen atoms with pressure is quite pronounced, and in the high-pressure phase, the two types of oxygens split in position at a greater rate than that associated with the lattice-parameter splitting. The Debye-Waller factor for the oxygen atoms shows a marked rise in the vicinity of the transition. These observations indicate that it is the motion of the oxygen atoms which is the driving force behind the transition.

II. TeO₂: EXPERIMENTAL

High-pressure neutron-diffraction measurements on TeO₂ were carried out at the CP-5 research reactor at Argonne using the piston-cylinder high-pressure apparatus with the time-of-flight diffractometer⁵ described previously. The sample material was powdered paratellurite, with a stated impurity level of less than 7 ppm, obtained from Alpha Inorganics. Three sets of measurements employing liquid pressure-transmitting media were made using two different liquids.

In the first two sets of measurements, the TeO₂ powder sample was wet-packed with liquid CS₂ into a Teflon capsule together with pellets of CsCl, which was used as a pressure calibrant. Each CsCl pellet was about $\frac{1}{16}$ in. thick and separated sections of the TeO₂ powder sample which comprised about 80% of the sample chamber volume. The capsule, with initial dimensions of 0.254-in. i.d. \times 0.303-in. o.d. \times 2 in. long, was sealed with an unsupported area-seal-type cap with an O-ring for making the low-pressure seal. The Teflon was surrounded by 0.002 in. of Pb foil in order to reduce friction with the cylinder walls. Good quality data was obtained for 13 pressures from 1 to 32.5 kbar. An orthorhombic distortion from the tetragonal unit cell of paratellurite, which was first observed at a pressure just above 9 kbar, exhibited a quadratic pressure dependence at all pressures up to 32.5 kbar. A good fit to the data in the high-pressure phase was obtained using the D_2^4 space group. The measurements using the CS₂ pressure fluid are only quasihydrostatic at pressures greater than $P=12.5$ kbar, where CS₂ solidifies at room temperature.⁶ The appearance of additional coherent scattering from solid CS₂ hampered the analysis of the data for the high-pressure phase which did not yield good values for atomic-position parameters. A measurement made on decreasing the pressure to $P=7.5$ kbar, after the TeO₂ had transformed to the high-pressure phase and after the CS₂ had solidified, showed no hysteresis in the TeO₂ lattice parameters. This is additional evidence that the transition is continuous.

Recent improvements on the inpile collimators which resulted in a fourfold gain in intensity led us to repeat the measurements in order to try to obtain good values for the position parameters in the high-pressure phase. Deuterated methanol, which remains fluid throughout the pressure range of our equipment,⁷ was used as the pressure medium. Excellent quality data at pressures up to 20 kbar were obtained. The values for position parameters showed a consistent variation

with pressure in both phases, with no discontinuity at the transition. Debye-Waller factors were also obtained in each phase.

Table I summarizes the lattice-parameter data from all three sets of measurements. Previous x-ray and neutron-diffraction data at room temperature and pressure are included for comparison. The rebuilding of the diffractometer in the period between the CS₂ and D-methanol runs resulted in a change in instrument calibration which led to a slight shift in the zero-pressure values for the TeO₂ lattice parameters. The most recent set of measurements showed less scatter due to improved statistics and the use of D methanol, so the figures and tables in the remaining sections include only the data from the final set of measurements. The $2\theta_B=60^\circ$ diffraction patterns for the measurement at $P=6.9$ kbar in the low-pressure phase and at $P=19.8$ kbar in the high-pressure phase are shown in Figs. 1 and 2. The solid curves show the least-squares profile refinements for the D_4^4 and D_2^4 space groups, respectively. The collimation provided by the steel binding ring eliminated diffraction peaks due to scattering from the pressure cell in the $2\theta_B=60^\circ$ pattern. The data for the $2\theta_B=30^\circ$ scattering angle included some pressure cell peaks, as well as one weak Teflon peak at 4.869 Å.

The use of hydrostatic pressure is important for this study. A preliminary set of measurements without a pressure fluid in which CsCl alone was used as the pressure medium showed a distortion at a much lower pressure than $P_c=9.0$ kbar reported by Peercy and Fritz,¹ and the data were of poor quality due to the nonuniform stress.

Each neutron-diffraction pattern was fit with a profile-refinement program using methods similar to those described previously.⁸ Our methods differ from those of Rietveld⁹ in several ways. We include three background parameters in our fitting function and include provisions for subtracting lines due to the pressure calibrant and/or the pressure cell. We have not included any corrections for preferred orientation, site occupancy, or peak asymmetry. These corrections would probably enable us to obtain a lower R value and improved accuracy, but since they do not change with pressure, their inclusion would not improve the precision of our measurement of pressure-dependent effects. Our room-temperature and pressure-position parameters for TeO₂ are in good agreement with measurements of Liecejewicz,¹⁰ as shown in Table II.

III. CELL DEFORMATION

The data at 19.8 kbar shown in Fig. 2 clearly show the splitting of all lines of the type (hkl) and

TABLE I. Lattice parameters of TeO₂.

<i>P</i> (kbar)	<i>a</i> (Å)	<i>b</i> (Å)	<i>c</i> (Å)	<i>V</i> (Å ³)
1. Cs ₂ medium				
0	4.8105(6)		7.6102(21)	176.11(9)
2.3(3)	4.8003(8)		7.5958(27)	175.03(12)
3.8(2)	4.7971(7)		7.5889(23)	174.64(11)
5.9(2)	4.7887(6)		7.5860(20)	173.96(9)
7.5(2)	4.7854(6)		7.5853(19)	173.70(9)
8.6(2)	4.7833(8)		7.5750(23)	173.31(10)
10.1(2)	4.7283(19)	4.8234(16)	7.5808(34)	172.89(20)
11.3(2)	4.6978(15)	4.8355(12)	7.5704(30)	171.97(17)
13.9(2)	4.6616(12)	4.8492(11)	7.5483(27)	170.63(14)
19.3(3)	4.6024(16)	4.8669(15)	7.5418(33)	168.93(18)
24.2(3)	4.5680(14)	4.8740(15)	7.5435(24)	167.95(16)
30.3(3)	4.5321(16)	4.8822(15)	7.5366(23)	166.76(16)
32.5(4)	4.5247(21)	4.8832(20)	7.5374(32)	166.54(22)
2. D-Methanol medium				
0	4.8052(3)		7.6021(8)	175.53(4)
4.2(2)	4.7911(3)		7.5868(8)	174.15(4)
6.9(2)	4.7833(2)		7.5729(8)	173.27(3)
9.8(2)	4.7418(9)	4.8051(9)	7.5632(10)	172.33(9)
11.4(2)	4.7085(7)	4.8234(7)	7.5525(11)	171.53(7)
13.6(2)	4.6753(8)	4.8366(8)	7.5468(13)	170.65(9)
16.6(2)	4.6410(7)	4.8504(7)	7.5364(12)	169.65(7)
19.8(2)	4.6053(6)	4.8557(6)	7.5300(10)	168.39(7)
3. Leciejewicz (neutron diffraction)				
0	4.796		7.626	175.41
4. Stehlik and Balak (x-ray diffraction)				
0	4.805		7.609	175.68

(*hk*0) but no splitting of lines of the type (*hhl*) which would occur if the transformation was of the type $a' = \sqrt{2}a$.¹¹ Except for the splitting mentioned no lines appeared or disappeared in either the $2\theta_B = 60^\circ$ or the $2\theta_B = 30^\circ$ patterns. The presence of any superlattice peaks at large plane spacings associated with an increase in unit-cell dimensions would have been evident in the $2\theta_B = 30^\circ$ pattern. The observed splitting means that the

transformation involved is merely a deformation of the unit cell, and the transition is a pure strain transition of the type discussed by Anderson and Blount¹² and by Boccara.²

Figure 3 shows the TeO₂ lattice parameters versus hydrostatic pressure to 20 kbar. The primary feature is the splitting of the tetragonal *a* lattice parameter into the unequal *a* and *b* orthorhombic parameters which begins at $P \sim 9$

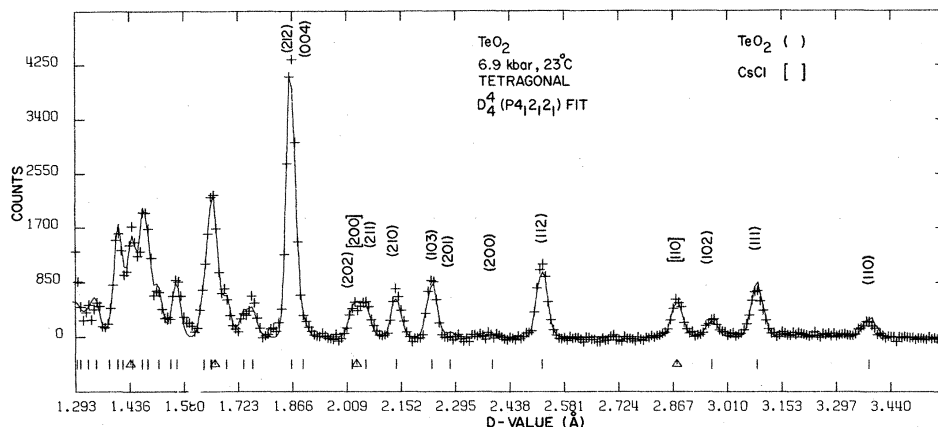


FIG. 1. Time-of-flight neutron-diffraction pattern of TeO₂ at 6.9 kbar and 23°C. The solid curve is the least-squares profile refinement using the D_4^4 space group. The pluses are the raw data points after subtraction of backgrounds. The vertical lines and triangles indicate the positions of the TeO₂ and CsCl peaks. Indexing of TeO₂ peaks is given in round brackets and of CsCl in square brackets.

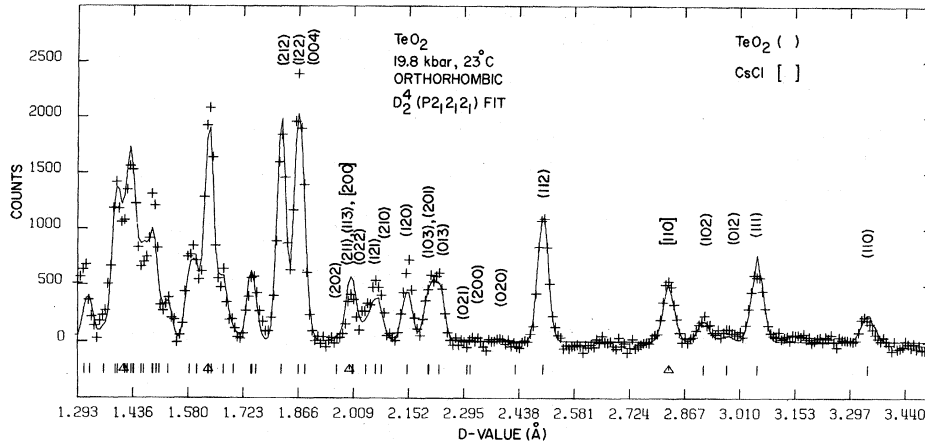


FIG. 2. Profile refinement of the 19.8 kbar pattern of TeO_2 . Note the splitting of lines of the type hkl while the lines of the type hhl show no splitting.

kbar and increases rapidly with pressure. The b parameter increases with pressure above 9 kbar and exceeds the room-pressure value of the tetragonal a at a pressure only 1 kbar above the transition. Two secondary features are evident. The quantity $(a+b)/2a_0$ shows a more rapid decrease with pressure in the high-pressure phase than does a/a_0 in the low-pressure phase. The c parameter shows a similar behavior with a more rapid decrease with pressure in the high-

pressure phase.

The anomalies in the pressure derivatives of the lattice parameters lead to an anomaly in dV/dP , as shown in Fig. 4. These slope discontinuities alone give only a rough indication of the transition pressure P_c which can be obtained

TABLE II. TeO_2 structural parameters at 1 bar and 19.8 kbar.

This work at 1 bar				
Atom	x	y	z	B
Te	0.025(1)
O	0.139(1)	0.262(1)	0.187(1)	0.63(15)
$a = 4.8052(3)$, $c = 7.6021(8)$, $V = 175.53(4)$.				
Leciejewicz at 1 bar (Ref. 10)				
Atom	x	y	z	B
Te	0.020(3)	0.0
O	0.142(2)	0.268(2)	0.182(2)	0.0
$a = 4.796$, $c = 7.626$, $V = 175.41$.				
Space group: $D_4^1(P4_12_12)$, Te atoms in $4a$ positions and oxygen atoms in $8b$ positions (Ref. 11).				
This work at 19.8 kbar				
Atom	x	y	z	B
Te	0.274(2)	0.012(3)	0.117(2)	0.0
O(1)	0.406(2)	0.234(2)	0.333(1)	1.08(16)
O(2)	0.549(2)	0.120(2)	0.940(1)	1.08(16)
$a = 4.6053(6)$, $b = 4.8557(6)$, $c = 7.5300(10)$, $V = 168.39(7)$.				
Space group: $D_2^4(P2_12_12)$ with origin as specified in Ref. 11. Atoms are in general positions ($4a$).				

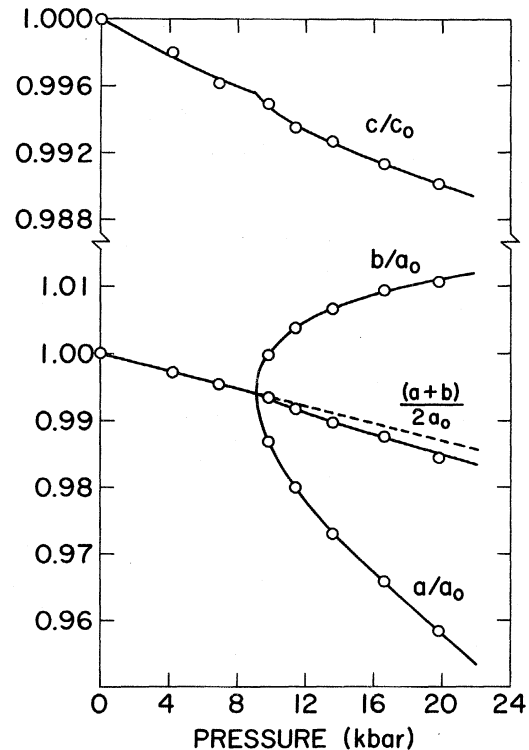


FIG. 3. Lattice parameters of TeO_2 vs pressure to 20 kbar. The solid curves are guides to the eye. The dashed line indicates the extrapolation of the tetragonal a value into the high-pressure phase region to indicate the change in slope of $(a+b)/2a_0$. Standard deviations are smaller than the points.

much more accurately from a plot of $(b-a)^2/a_0^2$ vs P and the extrapolation of the resulting straight line as shown in Fig. 4. A linear least-squares fit to these data yields $[(b-a)/a_0]^2 = -2.30(1) \times 10^{-3} + 2.53(1) \times 10^{-4} P$ (P in kbar). This goes to zero at a pressure of $P_c = 9.1(2)$ kbar, in good agreement with the elastic-constant measurements of Peercy and Fritz.¹

IV. SPACE GROUP AND ATOMIC DISPLACEMENTS

In Sec. III, we showed that the 9 kbar transition in TeO_2 is a transition involving a deformation of the unit cell from tetragonal to orthorhombic. The soft mode involved has been shown by Peercy and Fritz¹ to correspond to the effective elastic constant $\frac{1}{2}(C_{11} - C_{12})$. Boccara² has shown that in this situation, the point group must change from $D_4(422)$ to $D_2(222)$ and that the transition can be second order.

Of the D_2 space groups, observed selection rules in our powder-diffraction data rule out space groups $D_2^5 - D_2^9$. Space groups $D_2^1 - D_2^3$ allow extra lines which are not observed, and they can-

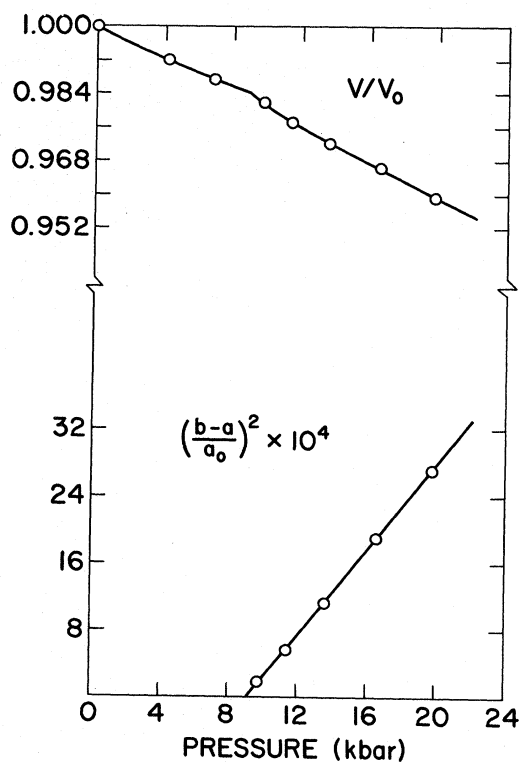


FIG. 4. V/V_0 and $[(b-a)/a_0]^2$ vs pressure. In the lower part of the figure, the solid straight line is the least-squares-fitting result $[(b-a)/a_0]^2 = -2.30(1) \times 10^{-3} + 2.53(1) \times 10^{-4} \times P$ (P in kbar). Standard deviations are smaller than the data points.

not be obtained by a small distortion of D_4^4 without large displacements of the atoms. The space group $D_2^4(P2_12_12_1)$ is the only remaining possibility for the high-pressure phase. We note that D_2^4 is a subgroup of D_4^4 and is therefore compatible with a second-order transition.

The starting values for the profile refinement of the high-pressure phase data with the D_2^4 space group were obtained from the low-pressure phase parameters by shifting the origin and relating the space-group operations in the two phases. The fractional translations associated with each rotational symmetry operation can be separated into components parallel and perpendicular to the rotation axis. The component parallel to the rotation axis is independent of the choice of origin. Comparison of the perpendicular components of the fractional translations for the operations in each space group as given in the International Tables¹¹ reveals that the origin of the unit cell for D_2^4 is shifted by $(\frac{1}{4}, 0, \frac{1}{8})$ from the D_4^4 origin. The unit cell showing the projection of the atoms on the x - y plane in the high-pressure phase is shown in Fig. 5. Table II lists the atomic-position parameters, lattice parameters, and Debye-Waller factors for the D_2^4 phase of TeO_2 at 19.8 kbar.

Figures 6 and 7 show the atomic-position parameters versus pressure to 20 kbar. Error bars

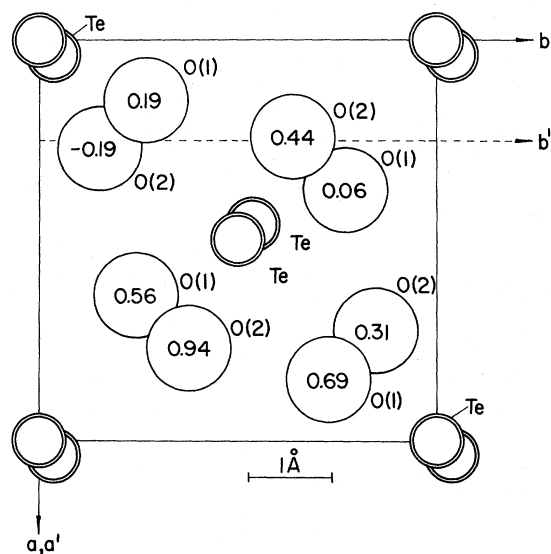


FIG. 5. Projection of the TeO_2 unit cell onto the x - y plane. The different choices of origin for D_4^4 and D_2^4 are indicated by the unprimed and primed a and b axes. The numbers inside the large circles representing the large oxygen atoms indicate typical values of the fractional z coordinates in the D_2^4 phase. There are twelve atoms in the primitive unit cell in both phases. The numbers in parentheses indicate which oxygen atoms are inequivalent in the high-pressure phase.

on the data points indicate the standard deviations obtained in the nonlinear least-squares fitting. These do not take into account systematic errors, but are a good indication of the precision of the measurements, except for the data at 9.8 kbar. Here the distortion only slightly broadens the lines, and the values for the position parameters affecting the relative intensities of the twinned lines are probably influenced by the fact that the individual peaks are not perfectly Gaussian. With the exception of the values at 9.8 kbar, the position parameters show a smooth change with pressure, which illustrates clearly the details of the transition process. The position parameters in the high-pressure phase have been plotted in such a way as to show their equivalence to the parameters in the low-pressure phase at the transition. The splitting of the x - y plane parameters is emphasized by the fact that they are given in fractional units of a and b , but the same type of splitting results for the oxygen atoms if the parameters are plotted in absolute units.

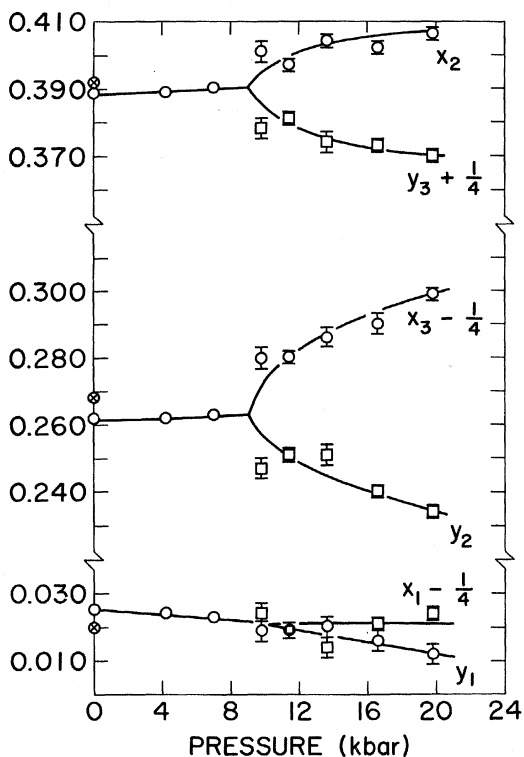


FIG. 6. Pressure dependence of the x and y atomic-position coordinates in TeO_2 in the D_4^h and D_2^h phases. x_1 and y_1 refer to the Te coordinates, while x_2 , y_2 refer to coordinates of O(1) and x_3 , y_3 refer to coordinates of O(2). The circles enclosing an x at $P=0$ are the values of Leciejewicz.¹⁰ Where not indicated by error bars, the standard deviations are smaller than the points. The points just above the transition are most uncertain because the diffraction lines were only slightly broadened.

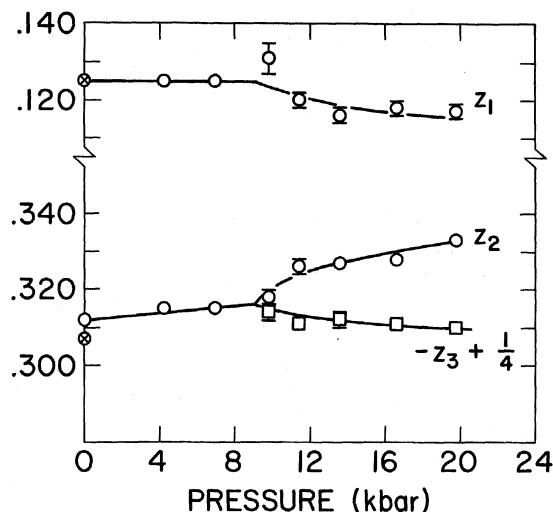


FIG. 7. Fractional z coordinates of the Te (z_1) and O (z_2 and z_3) atoms in the D_4^h and D_2^h phases of TeO_2 . In the low-pressure D_4^h phase, z_1 is fixed by symmetry at 0.125. The circled x 's are the values of Leciejewicz.¹⁰ Where not indicated by error bars, the standard deviations are smaller than the points.

From the pressure variation of the position parameters, it is clear that it is the motion of the oxygen atoms which is primarily responsible for the transition. This is also illustrated by the increase in the Debye-Waller factor for the oxygen atoms in the region of the transition, as shown in Fig. 8. The Debye-Waller factor for the

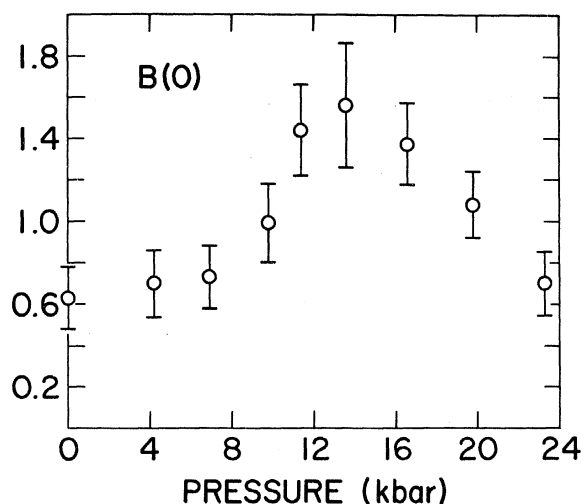


FIG. 8. Oxygen Debye-Waller factors obtained in the least-squares profile refinement of the TeO_2 data. Although the uncertainties are large, it is clear that there is an increase near the transition. The Te Debye-Waller factors were smaller than their standard deviations in all cases. Leciejewicz took both $B(\text{Te})$ and $B(\text{O})$ equal to zero in his fitting.¹⁰

Te atoms vanished in all fits to the data in both phases, indicating that the statistical uncertainty in this parameter is larger than its magnitude.

V. LANDAU THEORY FOR A PURE STRAIN TRANSITION

The elastic-constant measurements of Peercy and Fritz¹ indicate that the pressure-induced phase transition in TeO₂ is driven by the softening of the acoustic phonon mode with the effective elastic constant $\frac{1}{2}(C_{11} - C_{12})$. Recent inelastic neutron-scattering measurements¹³ show that complete softening of this mode is restricted to a narrow region at the Brillouin-zone center. From our neutron-diffraction measurements, an orthorhombic distortion ($b - a \neq 0$) of the tetragonal symmetry with no abrupt change in unit-cell dimensions sets in for $P > P_c$, so that $(b - a)^2$ varies linearly with pressure, going smoothly to zero as $P \rightarrow P_c$ from the high-pressure side. The foregoing is strong experimental evidence that the phase transition at $P_c = 9$ kbar in TeO₂ is a pure strain transition of the type discussed by Anderson and Blount¹² and by Boccara² in the framework of the Landau theory for continuous phase transitions.³ There are several symmetry requirements which must be obeyed. In Sec. IV, we showed that the space group in the high-pressure phase is D_2^4 , satisfying the requirement that the space group for the low-symmetry phase be a subgroup of the high-symmetry phase.¹⁴ The requirement that no third-order invariants can be formed from the order parameter is automatically satisfied in TeO₂, since the order of D_2^4 is one half the order of D_4^4 .² The transition can still be first order if the coefficient of the fourth-order term in the free-energy expansion is negative. In order for a strain component to be an order pa-

rameter, it must violate the symmetry of the high-symmetry phase.² In TeO₂, the soft mode is the twofold degenerate E mode, corresponding to the effective elastic constant $\frac{1}{2}(C_{11} - C_{12})$. These modes are infrared and Raman active. Since they are degenerate, the strain produced by them is caused by a combination of two symmetry-equivalent acoustic modes so that the symmetry of the strain is given by $E \times E = A_1 + A_2 + B_1 + B_2$. From the compatibility table,¹⁵ the symmetry of the strain in the low-symmetry phase must be $A_1 + B_1$, since in going from the high- to the low-symmetry-phase space group, $A_1, B_1 \rightarrow A_1$ and $A_2, B_2 \rightarrow B_1$.¹⁵

The soft mode of vibration condenses out at the transformation point resulting in a static distortion for which the static displacements must have exactly the symmetry properties of the soft mode. The primary order parameter is chosen accordingly and corresponds to the strain $\eta_1 = e_1 - e_2$, where e_1 and e_2 are strain components taken along the two equal axes of the tetragonal cell. This strain leads to a splitting of the tetragonal lattice parameter a into the unequal a and b axes of the orthorhombic cell. In addition to this distortion, we have observed small anomalies in $d[(a + b)/2a_0]/dp$ and in $d(c/c_0)/dp$ (Fig. 3). These anomalies are associated with $\eta_2 = e_1 + e_2$ and $\eta_3 = e_3$ strains, respectively, where e_3 is the strain component along the c axis. The latter two strains do not violate the tetragonal symmetry and therefore cannot represent primary order parameters. Fritz and Peercy¹⁶ have worked out the structural features for a transition characterized by the primary order parameter η_1 and one secondary order parameter η_2 . Extending their theory to include an additional secondary or induced order parameter η_3 , the expression for the elastic energy becomes

$$U = \frac{1}{2} \left[\frac{1}{2} (C_{11} - C_{12}) \eta_1^2 + \frac{1}{2} (C_{11} + C_{12}) \eta_2^2 + 2C_{13} \eta_2 \eta_3 + C_{33} \eta_3^2 \right] + \frac{1}{4} \left[\frac{1}{2} (C_{111} - C_{112}) \eta_2 \eta_1^2 + (C_{113} - C_{123}) \eta_3 \eta_1^2 \right] + \frac{1}{24} \left[\frac{1}{8} (C_{1111} - 4C_{1112} + 3C_{1122}) \eta_1^4 \right]. \quad (1)$$

Here we have kept terms up to fourth order in the primary order parameter and up to second order in the induced order parameters. In Fritz and Peercy's theory, the various elastic constants appearing in Eq. (1) are assumed to be pressure dependent, and thus for a given pressure, the quantities e_1, e_2, e_3 , or η_1, η_2 , and η_3 represent small deviations of the strains from their tetragonal phase values at that particular pressure. Using $\bar{\eta}_i$ to denote the equilibrium value of the i th

order parameter, the equilibrium configuration of the lattice in terms of the $\bar{\eta}_i$'s is

$$\begin{aligned} a &= a_T \left(1 + \frac{1}{2} \bar{\eta}_2 - \frac{1}{2} \bar{\eta}_1 \right), \\ b &= a_T \left(1 + \frac{1}{2} \bar{\eta}_2 + \frac{1}{2} \bar{\eta}_1 \right), \\ c &= c_T \left(1 + \bar{\eta}_3 \right), \end{aligned} \quad (2)$$

where a_T and c_T are the background tetragonal

phase lattice parameters at a particular pressure. For a particular pressure, the $\bar{\eta}_i$'s are found by minimizing the elastic energy U in Eq. (1) with respect to η_1 , η_2 , and η_3 . The trivial

$$\begin{aligned}\bar{\eta}_1^2 &= -(C_{11} - C_{12})\left[\frac{1}{2}(C_{11} + C_{12})C_{33} - C_{13}^2\right]/D = -(C_{11} - C_{12})(A/D), \\ \bar{\eta}_2 &= -\frac{1}{4}(C_{11} - C_{12})\left[C_{13}(C_{113} - C_{123}) - \frac{1}{2}C_{33}(C_{111} - C_{112})\right]/D = -\frac{1}{4}(C_{11} - C_{12})(B/D), \\ \bar{\eta}_3 &= \frac{1}{8}(C_{11} - C_{12})\left[(C_{11} + C_{12})(C_{113} - C_{123}) - C_{13}(C_{111} - C_{112})\right]/D = \frac{1}{8}(C_{11} - C_{12})(C/D),\end{aligned}\quad (3)$$

where

$$D = \frac{1}{8}(C_{111} - C_{112})B - \frac{1}{8}(C_{113} - C_{123})C + \frac{1}{8}\gamma A, \quad (4)$$

and

$$\gamma = \frac{1}{8}(C_{1111} - 4C_{1112} + 3C_{1122}). \quad (5)$$

The two secondary order parameters η_2 and η_3 are proportional to $(C_{11} - C_{12})$ and therefore can be written in terms of the primary order parameter η_1 . Eq. (3) becomes

$$\begin{aligned}\bar{\eta}_2 &= \frac{1}{4}(B/A)\eta_1^2, \quad \bar{\eta}_3 = -\frac{1}{8}(C/A)\eta_1^2, \\ \bar{\eta}_1^2 &= (A/D)\left[(C_{111} - C_{112})/(C_{11} + C_{12})\right](P - P_c),\end{aligned}\quad (6)$$

where in the last relation, Eq. (6), we have used Fritz and Peercy's result that in the vicinity of P_c the pressure dependence of $C_{11} - C_{12}$ is given by $-(C_{11} - C_{12}) = (C_{111} - C_{112})(P - P_c)/(C_{11} + C_{12})$. Several important features of our neutron-diffraction measurements are predicted by Eq. (6). First, the primary order parameter $\bar{\eta}_1^2 = [(b-a)/a_T]^2$ is linear in $P - P_c$ in the vicinity of P_c , as shown in Fig. 3. Second, there are two secondary order parameters $\bar{\eta}_2 = -(2/a_T) \times [a_T - (a+b)/2]$ and $\bar{\eta}_3 = -(1/c_T)(c_T - c)$ which are represented respectively by the slope change in $(a+b)/2a_0$ vs P and in c/c_0 vs P at the transition (Fig. 3). The linear dependence of η_2 on $P - P_c$ predicted by Eq. (6) is well born out experimentally for pressures up to 20 kbar. The pressure derivative of c/c_0 does increase on passing into the high-pressure phase (Fig. 3), verifying the existence of the order parameter η_3 , but the anomaly in c/c_0 vs P is too small to allow a meaningful determination of its pressure dependence.

VI. DISCUSSION

We have confirmed that the 9 kbar transition in TeO_2 is a pure strain transition causing a deformation of the unit cell of the type discussed by Anderson and Blount.¹² Elastic-constant measurements made to within 0.05 kbar of the transition extrapolate to a common pressure value.¹⁷ Any discontinuity in the soft-mode elastic constant must be less than 10^8 dyn/cm², which is three orders of magnitude below typical shear constants for ionic crystals.¹⁷ While this is still the most precise indication of the second-order nature of the transition, we have added strong evidence for a continuous transition by measuring the pressure dependence of the strain order parameter in the high-pressure phase and finding that it extracts linearly to zero at P_c . We have also found that the high-pressure structure is completely compatible with the symmetry requirements for a second-order transition and that all lattice parameters exhibit the behavior expected in a second-order transition.

We believe that it is now clear that TeO_2 undergoes a continuous transition at 9 kbar, going from the $D_4^4(P4_12_12)$ paratellurite structure to the $D_2^4(P2_12_12_1)$ structure. The transition is induced by the soft acoustic shear mode corresponding to $C' = \frac{1}{2}(C_{11} - C_{12})$, and the primary order parameter is $(b-a)/a_0$, which is the strain induced by the condensation of the C' shear mode. Both the strain and the shear mode velocity exhibit mean-field behavior over a wide pressure range. Small anomalies in the derivatives of $\frac{1}{2}(a+b)$ and c indicate that these are secondary order parameters involved in the transition. Measurements of Debye-Waller factors and atomic-position parameters indicate that it is the motion of the oxygen atoms which is the driving force behind the transition.

*Based on work performed under the auspices of the U. S. Energy Research and Development Administration.

¹P. S. Peercy and I. J. Fritz, Phys. Rev. Lett. **32**, 466 (1974).

²N. Boccara, Ann. Phys. **47**, 40 (1968).

- ³L. D. Landau and E. M. Lifshitz, *Statistical Physics* (Pergamon, London, 1958), Chap. XIV.
- ⁴K. Brugger, *Phys. Rev.* **133**, A1611 (1964).
- ⁵R. M. Brugger, R. B. Bennion, and T. G. Worlton, *Phys. Lett. A* **24**, 714 (1967).
- ⁶P. W. Bridgman, *Proc. Am. Acad. Arts Sci.* **74**, 399 (1942).
- ⁷G. J. Piermarini, S. Block, and J. D. Barnett, *J. Appl. Phys.* **44**, 5377 (1973).
- ⁸D. L. Decker, R. A. Beyerlein, G. Rault, and T. G. Worlton, *Phys. Rev. B* **10**, 5584 (1974).
- ⁹H. M. Rietveld, *J. Appl. Cryst.* **2**, 65 (1969).
- ¹⁰J. Leceijewicz, *Z. Kristall.* **116**, 345 (1961).
- ¹¹*International Tables for X-ray Crystallography*, (Kynoch, Birmingham, 1952), Vol. 1.
- ¹²P. W. Anderson and E. I. Blount, *Phys. Rev. Lett.* **14**, 217 (1965).
- ¹³D. B. McWhan, R. J. Birgeneau, W. A. Bonner, H. Taub, and J. D. Axe, *J. Phys. C* **8**, L81 (1975).
- ¹⁴G. Ya. Lyubarskii, *The Application of Group Theory in Physics* (Pergamon, Oxford, 1960).
- ¹⁵G. F. Koster, J. O. Dimmock, R. G. Wheeler, and H. Statz, *Properties of the Thirty Two Point Groups* (MIT, Cambridge, 1963).
- ¹⁶I. J. Fritz and P. S. Peercy, *Solid State Commun.*
- ¹⁷P. S. Peercy, I. J. Fritz, and G. A. Samara, *J. Phys. Chem. Solids* (to be published).